LBL-21279
Preprint

Submitted to Particle Accelerators

A Comparison of the Chasman-Green and Triple Bend Achromat Lattices

A. Jackson

March 1986

Prepared for the U.S. Department of Energy under Contract DE-AC03-76SF00098

LBL-21279
ESG-11

A COMPARISON OF THE CHASMAN-GREEN AND TRIPLE BEND ACHROMAT LATTICES*

A. Jackson

Lawrence Berkeley Laboratory
University of California
Berkeley, CA 94720

March 1986

*This was supported by the Director, Office of Energy Research, Office of High Energy and Nuclear Physics, High Energy Physics Division, U.S. Dept. of Energy, under Contract No. DE-AC03-76SF00098.

A COMPARISON OF THE CHASMAN-GREEN AND TRIPLE BEND ACHROMAT LATTICES*

A. Jackson

1. Introduction

The basic Chasman-Green or double focusing achromat (DFA) lattice, see Fig. 1, represents the most compact and economical of the structures used in low emittance electron storage rings. The main problem with this structure arises from the requirement to operate at zero (or slightly positive) chromaticity. This demands the use of strong sextupole fields, which drive third order structure resonances. These, in turn, place a restriction on the tune of the lattice, particularly in the radial plane. Unfortunately, the DFA structure, which, when operated in the low emittance mode has a fixed phase advance across the achromat, is not very flexible in this regard. We will show, for example, that it is not possible to design for high-beta insertions whilst maintaining the desired tune.

The triple bend achromat (TBA) structure utilizing combined function magnets, see Fig. 2, first described by Vignola as a candidate for the U.S. 6 GeV synchrotron radiation source,[1] is the logical extension of the DFA lattice. Adding an extra bending magnet within the achromat permits the designer to tailor the phase advance across the achromat and the beta value in the insertion region whilst maintaining the desired tune shift across the cell.

This paper details the difficulties with the DFA structure and shows how they are overcome in the TBA design. The principles are illustrated in two lattices which have been optimized for a 1.5 GeV synchrotron light source.

*This was supported by the Director, Office of Energy Research, Office of High Energy and Nuclear Physics, High Energy Physics Division, U.S. Dept. of Energy, under Contract No. DE-AC03-76SF00098.

2. The Chasman-Green Lattice

DFA structures are utilized in the VUV and XRAY rings (both operational) at the National Synchrotron Light Source,[2,3] and are the basis of the conceptual designs in proposals for higher energy synchrotron radiation sources both in the U.S.[4] and in Europe.[5] However, as beam emittance is pushed ever smaller, and the requirement to optimize the new sources for insertion devices is emphasized, so the relative inflexibility of this type of structure becomes apparent.

First we demonstrate that the radial phase advance between the centres of the dipoles forming the achromat is approximately 180°. (This should be intuitively obvious from the form of the beta-functions, or by noting that an electron trajectory starting with some angle and zero displacement in the middle of the first bend is focused back to the axis in the middle of the second bend.)

Consider a DFA lattice with the minimum possible emittance. Sommer[6] has shown that for this condition the beta value has a minimum given by

$$\beta_m = \sqrt{\frac{3}{320}} \cdot \ell_b \left[1 + \frac{47}{6720} \cdot \theta_b^2 - \cdots\right] \qquad (2.1)$$

at a distance into the magnet given by

$$S = \frac{3}{8} \ell_b \left[1 - \frac{1}{240} \theta_b^2 + \cdots\right] \qquad (2.2)$$

where ℓ_b is the length of the dipole and θ_b is its bend angle in radians. These features are illustrated in Fig. 3.

For the lattices considered here, θ_b is much less than unity, so the second and higher terms in the expansion can be ignored.

The phase advance between the position at which beta is a minimum and the symmetry point in the achromat (which we assume to be a thin quadrupole) can be found from

$$\Delta\mu_x = \int_0^{5/8\ \ell_b+q} \frac{ds}{\beta} \tag{2.3}$$

where q is the distance from the end of the dipole to the symmetry point. Note that the development of beta from β_m through a parallel ended dipole to the symmetry point is given by

$$\beta(s) = \beta_m + s^2/\beta_m \tag{2.4}$$

Then

$$\Delta\mu_x = \beta_m \int_0^{5/8\ \ell_b+q} \frac{ds}{\beta_m^2+s^2}$$

now

$$\int \frac{dx}{a^2+x^2} = \frac{1}{a}\tan^{-1}\left(\frac{x}{a}\right)$$

$$\therefore \qquad \Delta\mu_x = \tan^{-1}\left[\frac{5/8\ \ell_b+q}{\sqrt{3/320}\ \ell_b}\right] \tag{2.5}$$

Fig. 4 shows $\Delta\mu_x$ as a function of q/ℓ_b.

Note that so long as the argument in brackets in Eq. (2.5) is $>> 1.0$ then $\Delta\mu_x \approx 90°$.

Even when we deal with the case where the emittance is not minimum the same analysis holds. The expression for $\Delta\mu_x$ becomes

$$\Delta\mu_x = \tan^{-1}\left[\frac{(\text{some fraction of } \ell_b) + q}{\beta_{minimum}}\right]$$

For example if $[\ldots] > 5$, $\Delta\mu_x > 79°$. That is if the distance between β_{min} and the symmetry point is greater than $5\,\beta_{min}$, then the phase advance between the positions where beta is a minimum is greater than 158°. For practical designs in low emittance structures (where one has to leave space for sextupole magnets, etc.) the inequality is much greater and the total phase advance approaches 180°.

We now look at the phase advance between β_{min} and the symmetry point in the insertion region, that is, moving out of the achromat.

Consider two extreme examples of the matched solution in the insertion. One has a large beta value at the symmetry point, the other a very small value. Using exactly the same arguments as above it can be readily seen that the first solution (with high beta) has a phase advance of approximately 90° between the symmetry point in the insertion and the position where beta is a minimum. This means that the total phase shift across the cell for this optic is approximately 360°.

Similarly if the focusing between the symmetry point and the achromat is point-to-point, with a minimum at the symmetry point, the phase advance across the insertion is approximately 180°, and the resulting phase shift per cell is ~ 540°.

Thus we can write limits on the radial betatron tune of the low-emittance Chasman-Green structure with periodicity p ...

$$p \lesssim \nu_x \lesssim 1.5\ p$$

where

$$\nu_x = \frac{1}{2\pi}\,\mu_x$$

But where do we need to sit in tune space?

We know that all low emittance storage rings require strong sextupole magnets to correct the large chromaticity that results from the strong focusing in such lattices. The sextupole fields provide a large driving term for the third-order structure resonances, the effects of which are observed throughout the achievable tune range. It is therefore of paramount importance to choose a tune that is as far as possible from such resonance lines.

We have seen that the radial tune range of interest is:

$$p < \nu_x < 1.5\ p$$

The resonances which must be avoided are given by:

$$3\ \nu_x = np$$

and

$$2\nu_y + \nu_x = mp$$

where m and n are integers.

In the radial plane the more stringent constraint comes from $3\nu_x = np$. Within the tune range $p < \nu_x < 1.5\ p$, the resonances that must be avoided are given by $n = 3$ and $n = 4$. Arranging the radial tune to lie midway between these resonances gives:

$$\nu_x = 1\frac{1}{6}\ p\ . \qquad (2.6)$$

With this choice of ν_x, the optimum vertical tune is given by:

$$\nu_y = \frac{p}{4}\left(2m - 1\frac{1}{3}\right) . \qquad (2.7)$$

Now concentrate on structures with $p = 12$. Then the working point should be chosen close to $\nu_x = 14$, with $\nu_y \approx 2$, 8 or 14. The choice of vertical tune is determined by the requirements on β_y in the insertion region, and the necessity to keep the vertical chromaticity as small as possible. For wiggler and undulator magnet insertions a small value of β_y is usually required for both aperture and matching considerations. This implies a high vertical tune. However, a high tune demands more chromatic correction from the sextupole magnets, leading to a reduction in dynamic aperture. For these reasons the intermediate tune of $\nu_y \approx 8$ is chosen.

In order to pinpoint a desirable working point in tune space it is necessary to consider the injection process (which is optimum at a fractional tune of ~ 1/4), and to avoid structure resonances higher than order 3. In Fig. 5 we see that one such point is $\nu_x, \nu_y = 13.75, 7.75$, and it is to this working point that the DFA structure described below has been set.

The DFA structure described here was developed for the LBL Advanced Light Source.[7] The basic specification for the machine is a low emittance lattice ($\epsilon_0 < 1.0\times10^{-8}$ m-rad) with 12 insertion straight sections (each 6 m long), optimized for operation at 1.5 GeV but capable of operating anywhere in the range 0.75 to 1.9 GeV. Some minor changes have been made to the original design (the sextupole distribution was altered to enhance the chromatic behaviour of the lattice and a third sextupole family was added to improve the betatron amplitude dependent tune shift) otherwise the lattice is as described in Ref. 7. A short list of parameters is given in Table 1.

Figure 6 shows the usual lattice functions, β_x, β_y, and D through one unit cell of the lattice. Note that $\beta_x = 3.0$ m at the center of the insertion region. This is a consequence of tuning the structure to $\nu_x = 13.75$. Matched solutions with $\beta_x > 3.0$ m can readily be found but, for the reasons described above, the radial tune

decreases. For example if β_x is increased to 6.0 m, ν_x goes down to 12.68 and the effects of the $3\nu_x = 36$ resonance are much more pronounced. As a consequence the tune change with momentum increases dramatically and the momentum acceptance drops from 3% to 1%. This results in an unacceptably small Touschek lifetime.

The performance of the lattice with $\beta_x = 3.0$ m is described in Figs. 7 to 11.

Figure 7 shows the tune change as a function of momentum deviation. The tune change within the momentum range $-0.03 < \delta < +0.03$ is tolerable, and it transpires that this is about the minimum momentum acceptance necessary to achieve a reasonable Touschek lifetime.

Figure 8 shows the radial tune change as a function of the betatron amplitude, measured at the symmetry point in the insertion region, where $\beta_x = 3$ m. The equivalent vacuum chamber aperture at this point is 16 mm. Tune shift with betatron amplitude is particularly important in the injection process, where the newly injected bunch of electrons starts off with a large coherent betatron motion. This decreases under the influence of synchrotron radiation damping and the betatron tune values trace out the curve of Fig. 8. It is important that no major resonances are crossed during this procedure. The initial betatron amplitude in the injection process can be shown to be $\approx$8 mm. Figures 8 and 5 show that in this case the injection process is safe.

Figure 9 shows the radial phase space plot of a trajectory close to the betatron stability limit. The symmetry of this plot indicates that injection could be either into the inside or the outside of the ring.

Figure 10 shows the dynamic aperture of the DFA lattice (as measured at the symmetry point in the insertion region) for the ideal machine, i.e. one in which there are no displacement or magnet multipole errors.

Acceleration is provided by a single accelerating gap with a maximum voltage of 3.2 MV. It can be seen that the dynamic aperture is well matched to the vacuum aperture.

Figure 11 shows the dynamic aperture in the presence of systematic and random magnetic field errors for on-momentum electrons. It is seen that the aperture shrinks to dimensions smaller than the vacuum chamber. However it is still sufficient for injection and for gas scattering lifetimes significantly greater than the Touschek lifetime.

What we have shown above is that the DFA (or Chasman-Green) structure is a viable option for a 1.0 to 2.0 GeV synchrotron radiation source. The weakness is its inflexibility in the range of radial beta values that can be accommodated in the insertion region.

3. The Triple Bend Achromat Lattice

Triple bend structures are utilized in both the ALADDIN[8] and BESSY[9] synchrotron radiation sources. The ALADDIN structure does not provide zero dispersion in its long straight sections and was not designed under the procedures described below. Rather, it is a machine optimized primarily to use radiation from the dipole magnets (not insertion devices) and has, as a specific design feature, the same lattice functions in each dipole magnet. BESSY, too, is designed to exploit dipole radiation, though its structure does have zero dispersion in the insertion straight sections. In this lattice, significant focusing in the vertical plane is provided by the edge angles of the dipoles. This focusing is necessary in order to constrain the amplitude of the vertical beta function.

When the machine periodicity is increased from $p = 4$ (BESSY), to $p = 12$ (ALS), the edge focusing becomes much weaker and it is necessary to introduce extra

vertical focusing. In the examples that follow, this was accomplished by including a gradient into the bending magnet fields.

A unit cell of the basic triple bend achromat lattice is shown in Fig. 2. The addition of the third bend in the achromat frees the lattice from the restriction on tune shift across the achromat. In fact the tune shift can be varied between 180° and 360° by changing the position of the achromat quadrupoles and/or the length of the central magnet compared to the outer magnets. (We assume equal fields in the bends since these are set to the technical limit for top energy operation.)

Let us illustrate these two points separately.

In Fig. 12 we show schematically two examples of the triple bend achromat structure for machines with the same periodicity, i.e., the sums of the bending angles per achromat are the same. The achromat quadrupoles are placed midway between the ends of the "three" magnets in each case. In Fig. 12a the center bend angle is zero times the outer bend angles and the lattice is similar to the Chasman-Green structure described above. The phase advance across the achromat is ~ 180° and there is a minimum emittance given by (ref. 2)

$$\varepsilon_m = 9.5\times10^{-8}\ \frac{E^2[\mathrm{GeV}]\theta_b^3}{J_x}\ \mathrm{m\text{-}rad}\ .$$

where J_x is the radial damping partition number. For a structure with energy E = 1.5 GeV, periodicity p = 12, and J_x = 1.0,

$$\varepsilon_m = 3.8\times10^{-9}\ \mathrm{m\text{-}rad}\ .$$

Figure 12b shows a structure in which the center bend angle (or length) is twice the

outer bend angle (length). In this case the dispersion falls to zero in the middle of the central bend and its magnitude and slope in the bends are everywhere smaller, leading to a smaller emittance. In fact the structure can be thought of as two DFA achromats (with half the total bend each) joined together. Thus the phase change across the achromat is approximately 360° and the minimum emittance for the structure might be expected to be about 8 times smaller (i.e., 0.5^3) than the structure shown in Fig. 12a.

Now consider the case where the lengths of the three bends are equal (see Fig. 13), each having 2/3 the bending angle of the magnets in Fig. 12a. Then the minimum emittance will be about one third of the minimum emittance of the DFA structure. If the achromat quadrupoles are placed at position A in the lattice the dispersion will go to zero in the middle of the central bend and the phase change across the achromat is at its maximum, i.e., close to 360°. If the achromat quadrupoles are moved towards the center of the achromat, say to position B, the dispersion match demands that the dispersion in the middle of the center bend increase from zero. (This is because D' at the exit from each magnet is independent of the position of the quadrupoles.) The strength of the quadrupole goes down (since it produces the same deflection at a greater distance from the axis), the emittance goes up (since there is now a larger dispersion in the center bend) and the phase advance across the achromat goes down (because there is less focusing).

These are the features of the TBA structure that allow the designer to tailor a structure to his particular needs. For example, let us look at a lattice with 12 superperiods, high radial beta in the insertion region (say 11 m), a low emittance (at least as small as the DFA structure described in section 2), and a radial tune of about 14.25 (in order to avoid the third order structure resonances). These specifications cannot simultaneously be met by the basic DFA structure.

The design procedure for the TBA lattice is as follows:

The phase advance across a unit cell is about 428°.

Since beta is large in the insertion, the phase advance from the symmetry point to approximately the middle of the outer bends is about 90°.

Thus the phase advance across the achromat must be adjusted to ~248° by judicious positioning of the achromat quadrupoles.

The result is the structure shown in Fig. 14, together with the usual lattice functions. The unit cell is only 0.5 m longer than the DFA cell. A short list of parameters is given in Table 2.

Note that vertical focusing has been introduced into the bending magnets. This is primarily to keep the vertical beta function under control. However, it also has the fringe benefits that it changes the damping partition parameters of the structure in such a way as to improve the emittance and produces beneficial separation of the radial and vertical beta functions in the region where one would like to place the chromatic sextupoles.

The analysis of the lattice performance follows that applied to the DFA structure and is presented in Figures 15 through 19.

Figure 15 shows a much improved momentum acceptance, with a tolerable tune variation within the range $-0.05 < \delta < +0.05$. The implication is that the Touschek lifetime will be significantly better than that of the DFA lattice. This was confirmed when a comparative study of lattice performance was made for candidate ALS structures.[10)]

Figure 16 shows a tune shift with betatron amplitude that is very close to that of the DFA structure, despite the fact that there are only two families of sextupoles.

The radial phase space plots in Fig. 17 confirm that injection can be performed from either inside or outside for this structure also.

The dynamic aperture for the ideal TBA structure, shown in Fig. 18, is marginally larger than the DFA structure. The corresponding acceptances (radial and vertical) are approximately equal and are slightly larger than the minimum acceptance (vertical) of the DFA lattice.

Finally we show the dynamic aperture for on-momentum electrons when magnet field errors are introduced, Fig. 19. The conclusions are the same as for the DFA structure, i.e., there is a reduction in aperture, but not sufficient to seriously degrade the performance of the lattice.

In conclusion then, we have shown that the TBA structure represents a more flexible option than the DFA structure in the design of low emittance storage rings. The distinguishing features of the structure are its intrinsically smaller emittance and the ability to choose the tune of the lattice and the beta values in the insertions independently. The weakness is that once these values are chosen (by fixing the geometry of the dipoles and quadrupoles) the tunes and beta values can only be varied over a small range. This inflexibility is addressed in the next section.

4. Variations on a Theme (Part 1)

One way of providing a "movable quadrupole" with fixed magnet geometry is to include a second family of quadrupoles between the bending magnets as shown in Fig. 20. By differentially powering these magnets one can generate an equivalent single quadrupole with a position anywhere between the fixed quadrupole positions. This allows the beta values in the insertions to be changed whilst maintaining the radial betatron tune. The price to be paid is in the emittance. If beta is reduced in the insertion straight, thereby increasing the phase advance across this region, the phase

advance across the achromat must be reduced to maintain the radial tune. This requires a reduction in the focusing strength in the achromat which increases the dispersion in the central bend and so increases the emittance.

This approach has been tested by adding an extra family of quadrupoles to the TBA structure described above and matching the structure to a radial beta value of 3.0 m at the symmetry point of the insertion straight, whilst preserving the radial tune of ~ 14.25. (Remember that with the new family of quadrupoles set to zero the structure reverts to the TBA lattice above with a beta value at the symmetry point of 11.0 m.) The resulting structure and lattice functions are shown in Fig. 21.

As expected the emittance increases, in this case to $\varepsilon_0 = 9.0 \times 10^{-9}$ m-rad.

The performance of this structure was analyzed in the same manner as previous structures. It behaves much like the basic TBA lattice with the exception of the radial acceptance, which is three times larger.

It is also possible to match adjacent insertions to different beta values whilst keeping the radial tune fixed. An example of such a solution is shown in Fig. 22. The emittance in this case suffers even more, increasing to $\varepsilon_0 = 13.9 \times 10^{-9}$ m-rad. A more aesthetically pleasing solution to the production of differential betas is discussed in the next section.

5. Variations on a Theme (Part 2)

A desirable feature of any lattice would be the capability to tailor the beta values in each straight section for a particular application whilst keeping the overall betatron tunes far from structure resonances. This could be achieved in the TBA structure by using quadrupole triplets to match into the insertion regions, rather than the doublets employed in the lattices described above, and powering each quadrupole around the ring independently.

Usually it is not necessary to introduce such a high degree of flexibility! What is required is the capability to change the radial beta-function between two values (high/low) in a pattern which keeps as high a periodicity, p, as possible.

This can be accomplished in the TBA structure by introducing triplet matching into every other insertion straight section. Such a solution, with the radial beta values set alternately to 11.0 m and 3.0 m is shown in Fig. 23. The free straight section length has been kept at 6.0 m and the addition of the extra quadrupoles adds 9.0 m to the circumference giving a total of 197.4 m. The emittance of this arrangement is $\varepsilon_0 = 5.4 \times 10^{-9}$ m-rad.

Lower periodicity structures can also be accommodated using this magnet arrangement. If we denote a high beta insertion by 'H', and low beta by 'L', the following solutions could be instituted:

H H H H H H H H H H H H	p = 12
H L H L H L H L H L H L	p = 6
H L H H L H H L H H L H	p = 4
H H H L H H H L H H H L	p = 3
H H H H H L H H H H H L	p = 2
H H H H H H H H H H H L	p = 1

This should be sufficient to meet most machine/user requirements.

6. Conclusions

We have shown that both the DFA and TBA structures represent viable alternatives for the lattice of a synchrotron radiation source designed for operation in the 1 to 2 GeV energy range. The performance of both structures is dominated by the influence of third-order structure resonances, which are driven by the strong sextupole fields necessary for chromatic correction. In the case of the DFA lattice, the resulting

constraints on the radial betatron tune severely limit the flexibility of the structure. The addition of the extra bend in the basic TBA structure permits the designer to decouple the beta functions in the insertion region from the betatron tune, at little cost in circumference, whilst taking advantage of the intrinsically lower emittance. By adding two more families of quadrupoles to the basic structure, as described in sections 4 and 5, it is possible to develop the basic TBA into a highly flexible lattice.

7. Acknowledgments

I would like to thank Gaetano Vignola for introducing me to the TBA structure and for many useful discussions, and Al Garren for a particularly well-focused comment which led to my understanding of the potential advantages of the structure.

In the process of this study extensive use has been made of various lattice matching and tracking codes, and in each case one or more of their authors has come to my aid in times of crisis. I am therefore grateful to Al Garren for help with SYNCH, Dave Douglas for help with MARYLIE, Roger Servranckx and Lindsay Schachinger for help with DIMAT, and Martin Donald for help with HARMON.

8. References

1. G. Vignola, Preliminary Design of a Dedicated 6 GeV Synchrotron Radiation Storage Ring, Nuclear Instruments and Methods A236 (1985) 414.

2. L. Blumberg et al., NSLS VUV Storage Ring, IEEE Trans. Nucl. Sci. NS-26 3842 (1979).

3. S. Krinsky et al., Design Status of the NSLS XRAY Storage Ring, IEEE Trans. Nucl. Sci. NS-26 3806 (1979).

4. 6 GeV Synchrotron X-Ray Source, Conceptual Design Report, ANL-86-08 (1986).

5. B. Buras and S. Tazzari, European Synchrotron Radiation Facility, Report of the ESRP, 1984.

6. M. Sommer, Optimization of the Emittance of Electron Storage Rings, Laboratoire de l'Accélérateur Linéaire LAL/RT/83-15 November 1983.

7. The Advanced Light Source: Technical Design, Lawrence Berkeley Laboratory, Pub-5111, Appendix A, May 1984.

8. E. Rowe et al., Status of the Aladdin Project, IEEE Trans. Nuc. Sci., Vol. NS-28, No. 3 3145 (1981).

9. D. Einfeld and G. Mülhaupt, Choice of the Principal Parameters and Lattice of BESSY, Nucl. Instr. and Meth. 172 (1980).

10. M. Cornacchia et al., Comparison of Lattice Options for a 1-2 GeV Synchrotron Light Source, to be published.

Table 1. Double Focusing Achromat Lattice - Short list of Parameters

Circumference	182.4 m
Emittance ε_0 (1.5 GeV)	0.9×10^{-8} m-rad
Betatron tune ν_x/ν_y	13.782/7.775
Natural chromaticity ξ_x/ξ_y	-32.0/-17.5
Max. strength of quadrupoles k1 max	$3.61\ m^{-2} \equiv 18.06$ T/m @ 1.5 GeV
Max. strength of sextupoles $\int$ k2 ds	$28.0\ m^{-2} \equiv 250\ T/m^2$, l = 0.28 m
Dipole field	1.6 T @ 1.9 GeV, 1.26 T @ 1.5 GeV
Momentum compaction factor	1.55×10^{-3}
RF harmonic	304

Table 2. Triple Bend Achromat Lattice - Short list of Parameters

Circumference	188.4 m
Emittance ε_0 (1.5 GeV)	0.4×10^{-8} m-rad
Betatron tune ν_x/ν_y	14.305/8.237
Natural chromaticity ξ_x/ξ_y	-24.5/-26.6
Max. strength of quadrupoles k1 max	$2.58\ m^{-2} \equiv 12.92$ T/m @ 1.5 GeV
Max. strength of sextupoles $\int$ k2 ds	$22.9\ m^{-2} \equiv 204.5\ T/m^2$, l = 0.28 m
Combined function magnets, B_0	1.6 T @ 1.9 GeV, 1.26 T @ 1.5 GeV
Field index, n	16.0 ≡ 4%/ cm
Momentum compaction factor	1.47×10^{-3}
RF harmonic	314

FIGURE CAPTIONS

Fig. 1. Basic DFA structure.

Fig. 2. Basic TBA structure.

Fig. 3. Features of the basic DFA structure tuned for minimum emittance.

Fig. 4. Phase advance from the position where $\beta = \beta_{min}$ to the achromat symmetry point.

Fig. 5. Resonance diagram up to order 6 showing the working point of the DFA structure.

Fig. 6. DFA - Structure and lattice functions.

Fig. 7. DFA - Betatron tune as a function of momentum.

Fig. 8. DFA - Radial tune shift with betatron amplitude, measured at the insertion symmetry Point.

Fig. 9. DFA - Radial phase space close to the stability limit.

Fig. 10. DFA - Dynamic aperture.

Fig. 11. DFA - Dynamic aperture in the presence of magnet field errors. (The statistical uncertainty along the x-axis is also shown.)

Fig. 12(a) TBA structure with a zero center bend angle.

Fig. 12(b) TBA structure with $\theta, 2\theta, \theta,$ magnet arrangement.

Fig. 12. Two examples of the TBA structure. 12(a) has a phase advance across the achromat $\approx \pi$ (it is a DFA lattice in disguise!). 12(b) is tuned to have a radial focus in the central bend (for low emittance) and has a phase advance approaching 2π across the achromat.

Fig. 13. TBA - Dependence of the matched dispersion function D on the position of the achromat quadrupoles. As the quadrupoles are moved from position A to C the strength required to match the dispersion function reduces.

Fig. 14. TBA - Structure and lattice functions.

Fig. 15. TBA - Betatron tune as a function of momentum.

Fig. 16. TBA - Radial tune shift with betatron amplitude, measured at the symmetry point in the insertion region.

Fig. 17. TBA - Radial phase space trajectories.

Fig. 18. TBA - dynamic aperture.

Fig. 19. Dynamic aperture in the presence of magnetic field errors. The statistical uncertainty along the x-axis is shown.

Fig. 20. TBA with two families of achromat quadrupoles. By differentially powering QF1 & QF2 it is possible to create the same dispersion in the central bend as those shown in Fig. 12.

Fig. 21. TBA with two quadrupole families/achromat.

Fig. 22. TBA with β_x tuned to different values in alternate straight sections.

Fig. 23. TBA employing triplet matching in alternate straight sections.

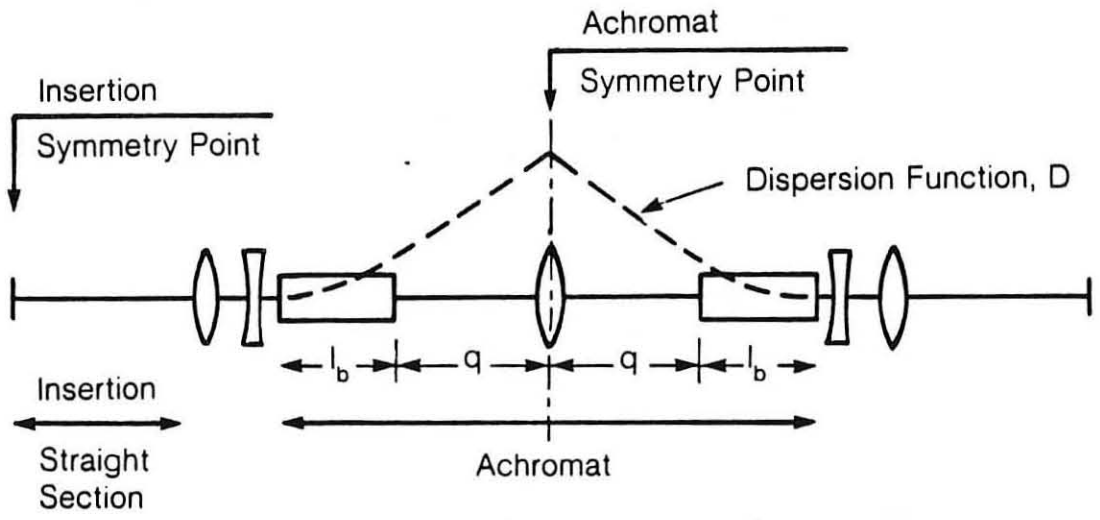

Fig. 1. Basic DFA structure.

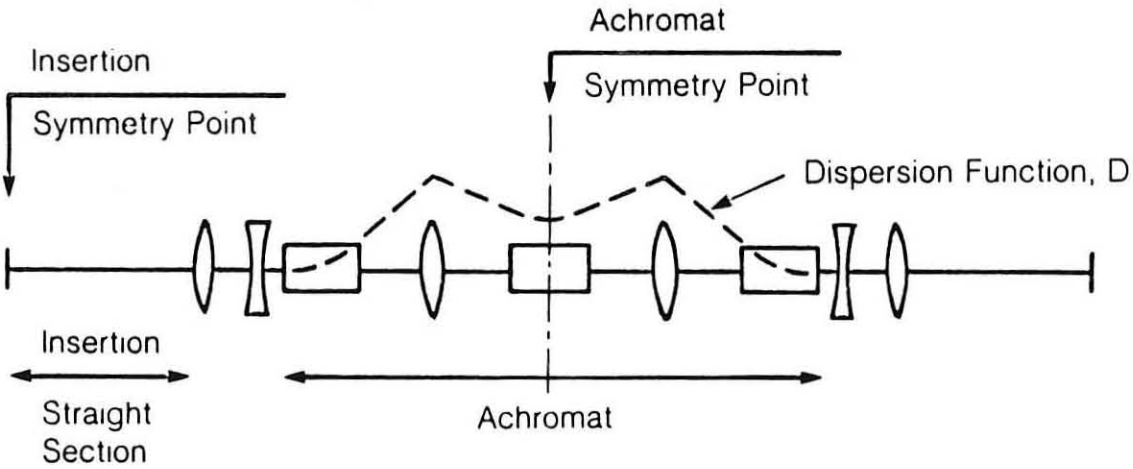

XBL 862-9598

Fig. 2. Basic TBA structure.

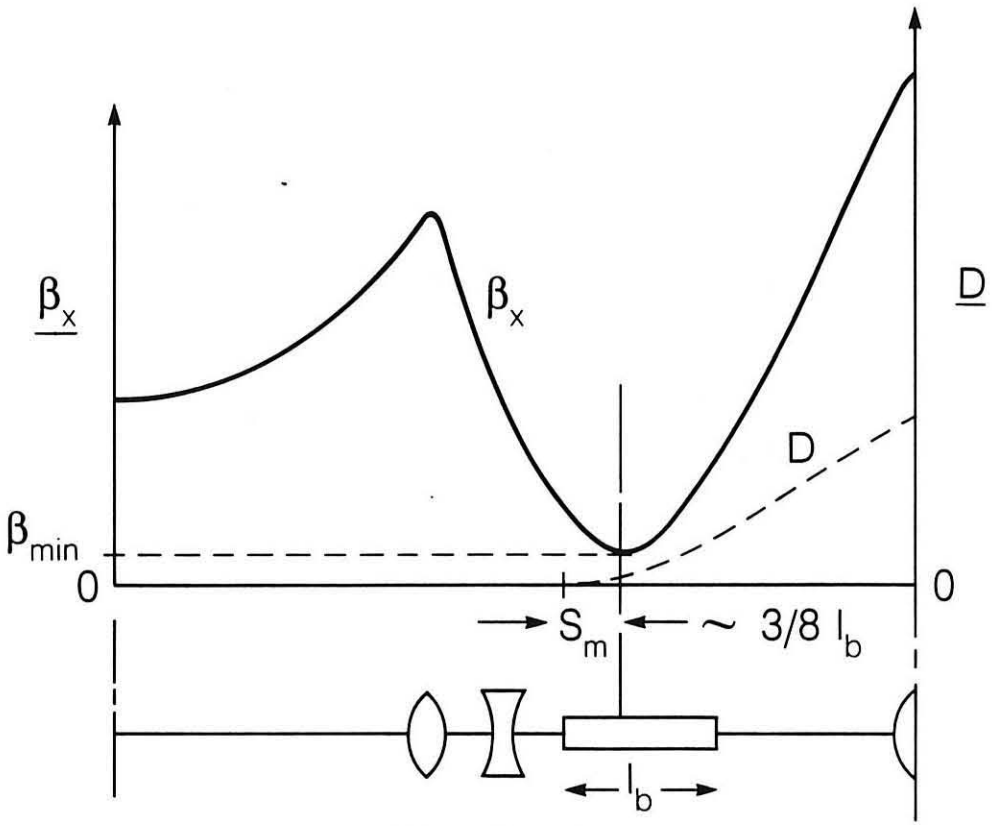

1/2 unit cell

$$\beta_{min} = \sqrt{\frac{3}{320}} \cdot l_b \left[1 + \frac{47}{6720} \cdot \Theta_b^2 - \cdots \right]$$

$$S_m = \frac{3}{8} \cdot l_b \left[1 - \frac{1}{240} \cdot \Theta_b^2 + \cdots \right]$$

Where Θ_b is the bending angle through l_b

XBL 862-9763

Fig. 3. Features of the basic DFA structure tuned for minimum emittance.

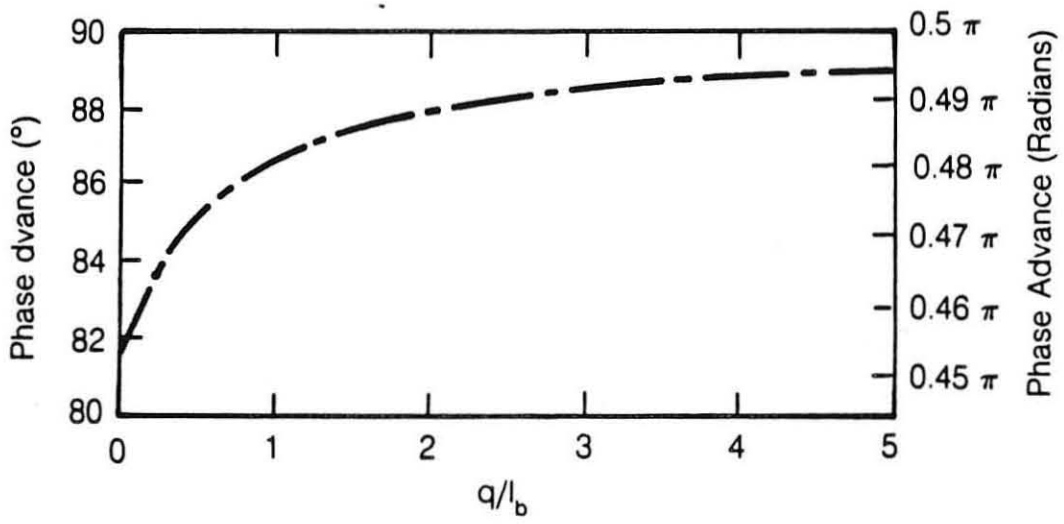

XBL 862-9599

Fig. 4. Phase advance from the position where $\beta = \beta_{min}$ to the achromat symmetry point.

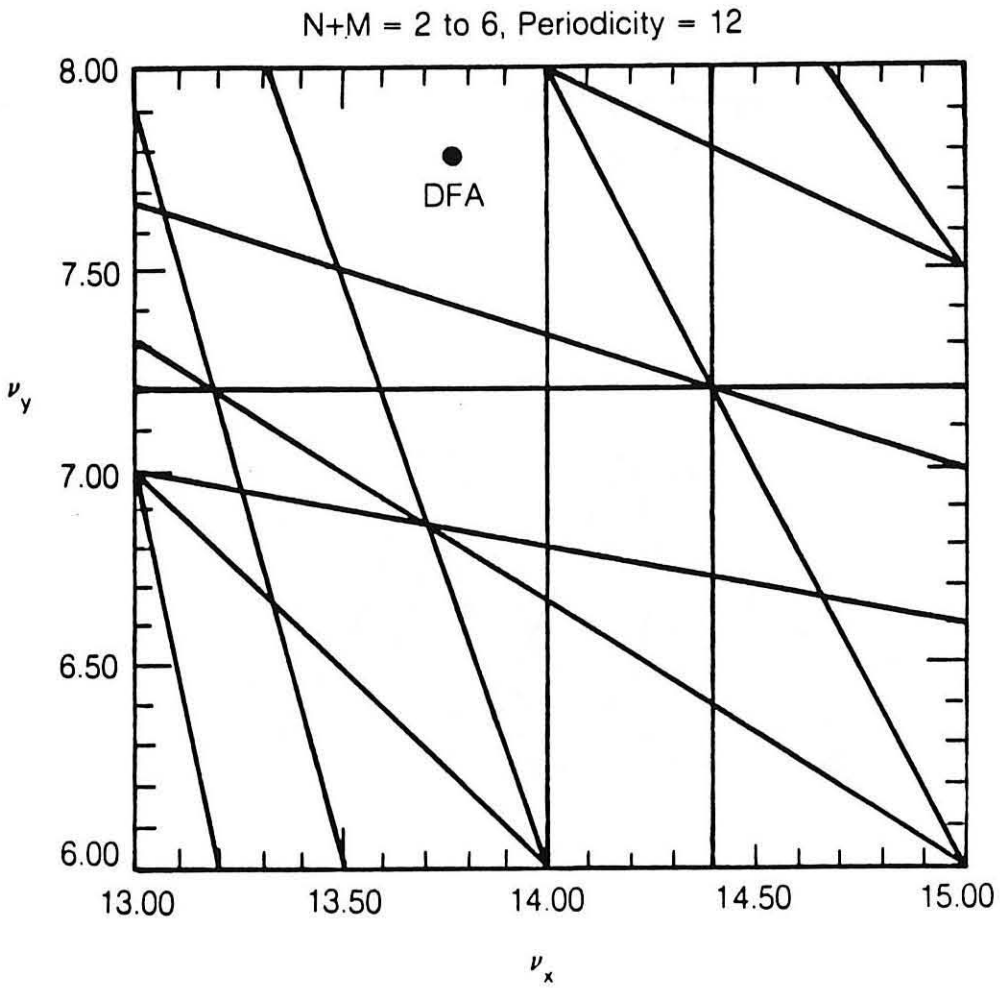

Fig. 5. Resonance diagram up to order 6 showing the working point of the DFA structure.

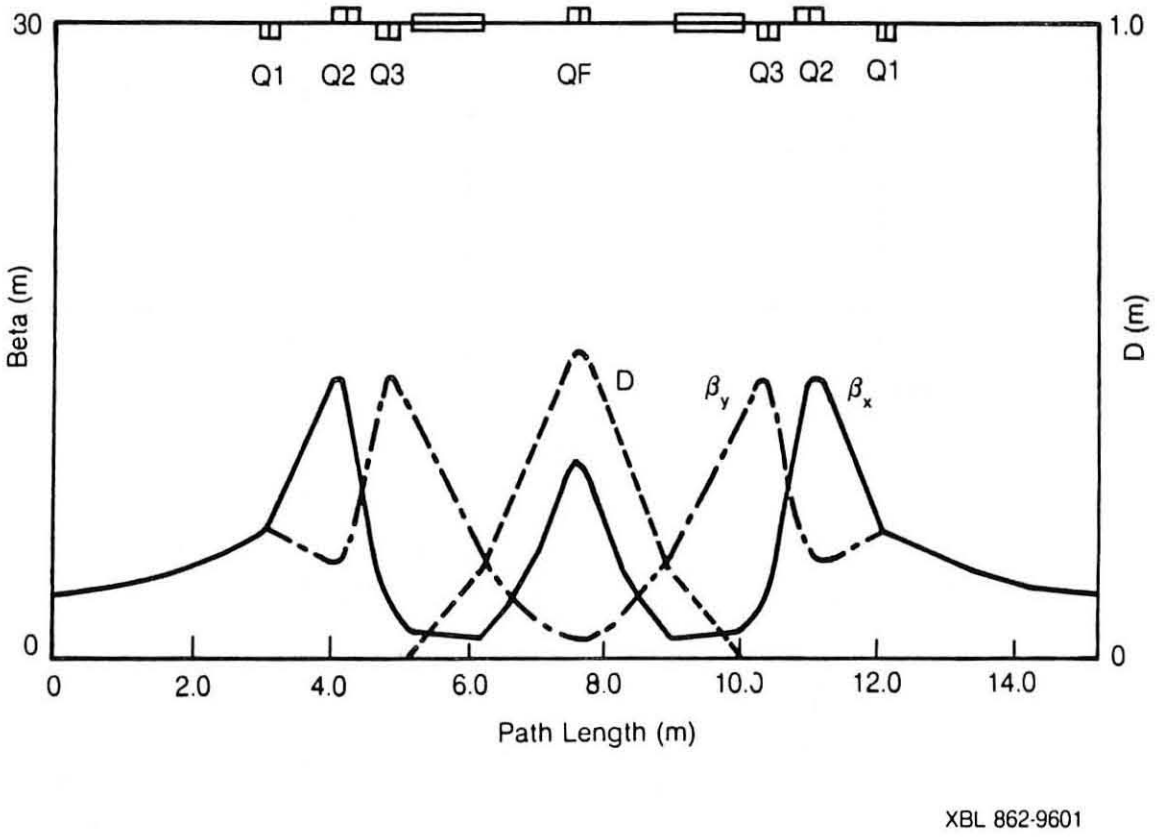

Fig. 6. DFA - Structure and lattice functions.

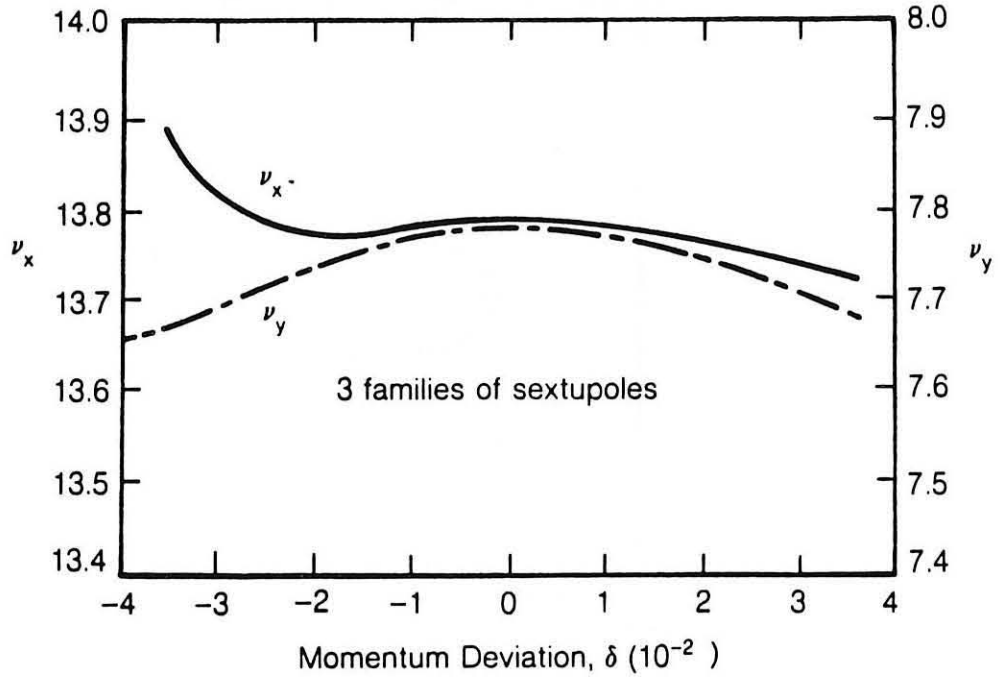

Fig. 7. DFA - Betatron tune as a function of momentum.

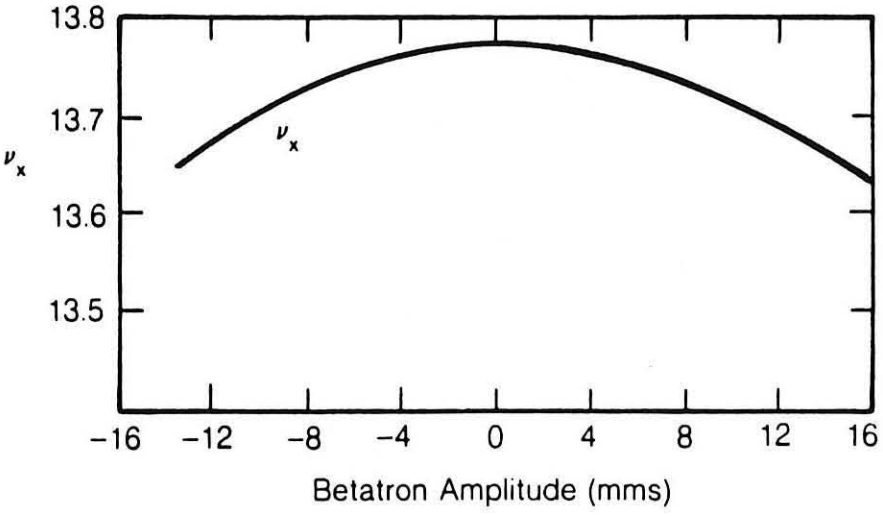

XBL 862-9612

Fig. 8. DFA - Radial tune shift with betatron amplitude, measured at the insertion symmetry Point.

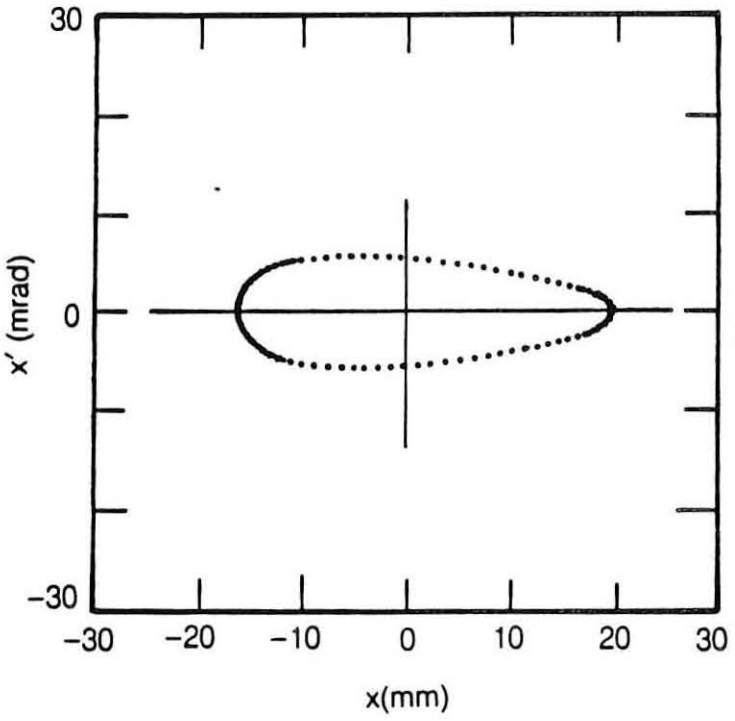

Fig. 9. DFA - Radial phase space close to the stability limit.

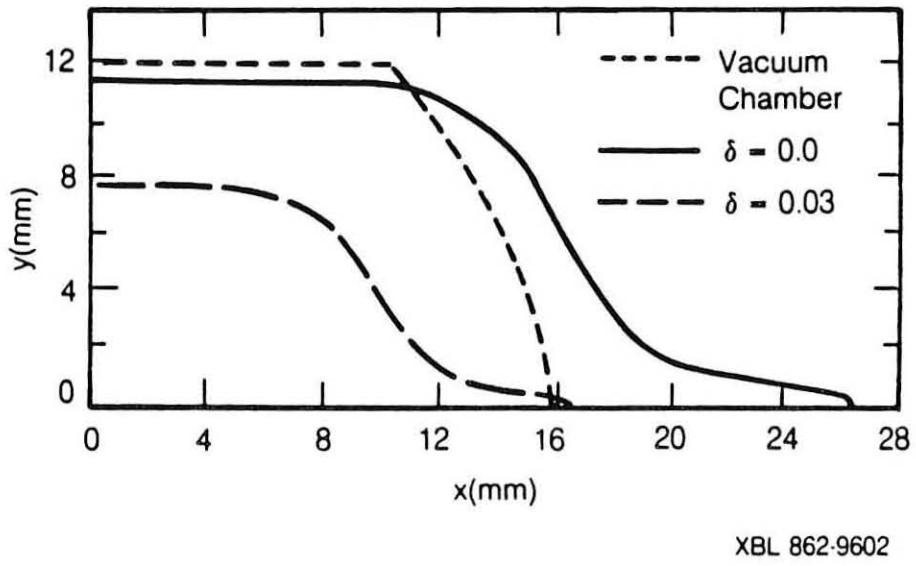

Fig. 10. DFA - Dynamic aperture.

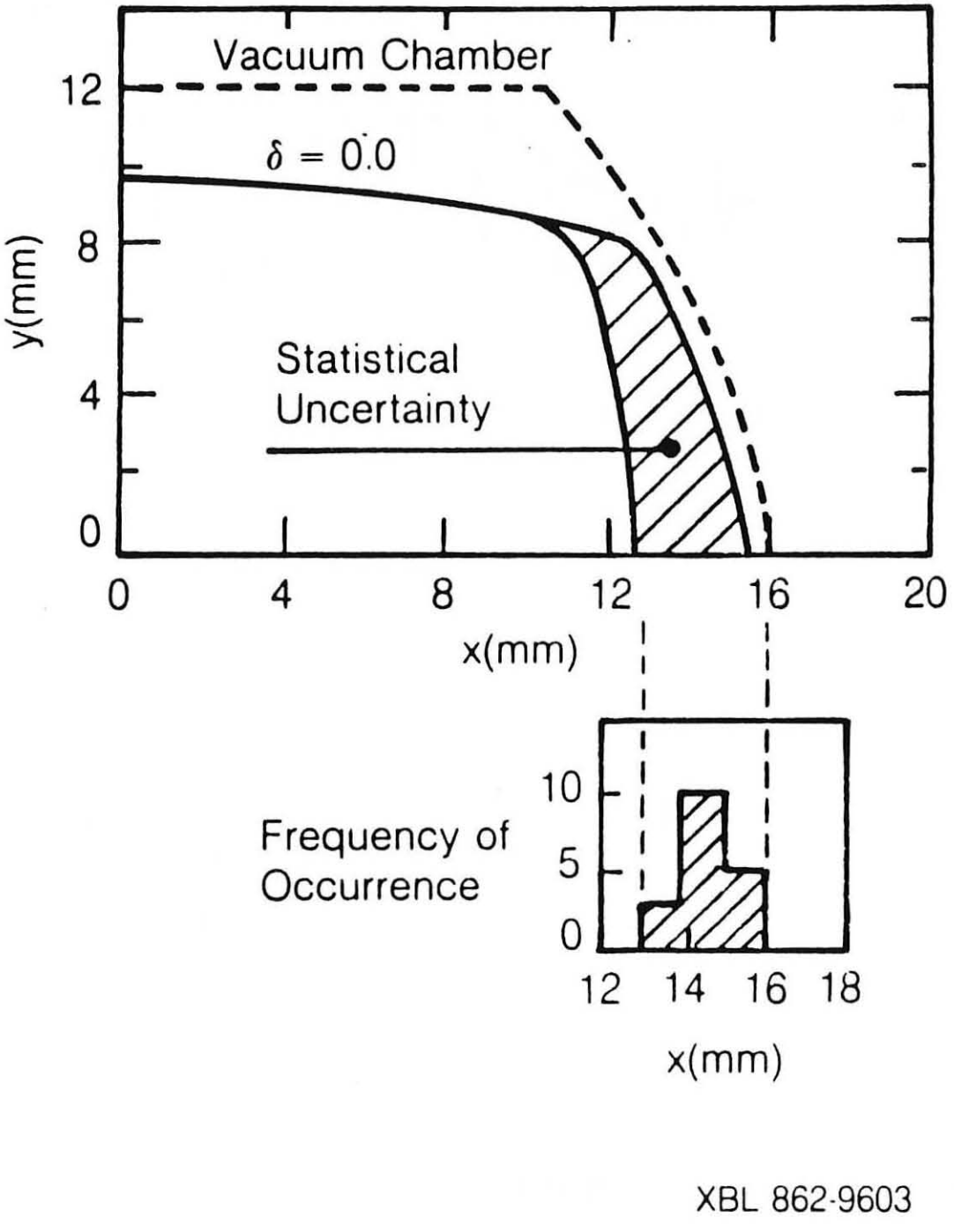

Fig. 11. DFA - Dynamic aperture in the presence of magnet field errors. (The statistical uncertainty along the x-axis is also shown.)

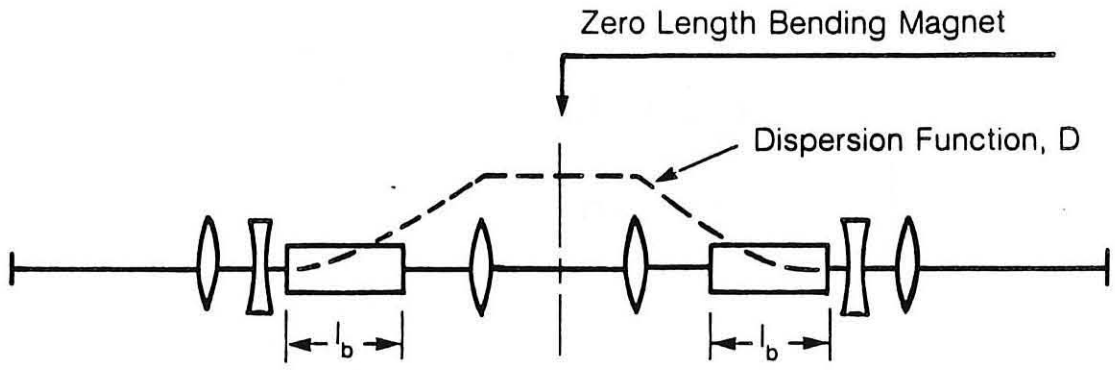

Fig. 12(a) TBA structure with a zero center bend angle.

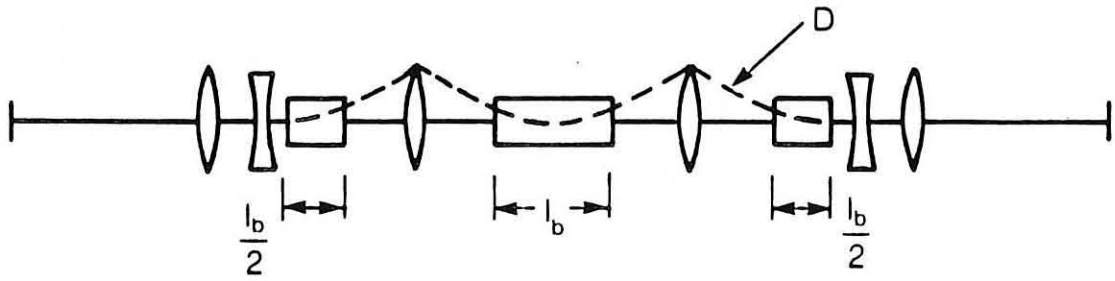

XBL 862-9604

Fig. 12(b) TBA structure with $\theta, 2\theta, \theta,$ magnet arrangement.

Fig. 12. Two examples of the TBA structure. 12(a) has a phase advance across the achromat $\approx \pi$ (it is a DFA lattice in disguise!). 12(b) is tuned to have a radial focus in the central bend (for low emittance) and has a phase advance approaching 2π across the achromat.

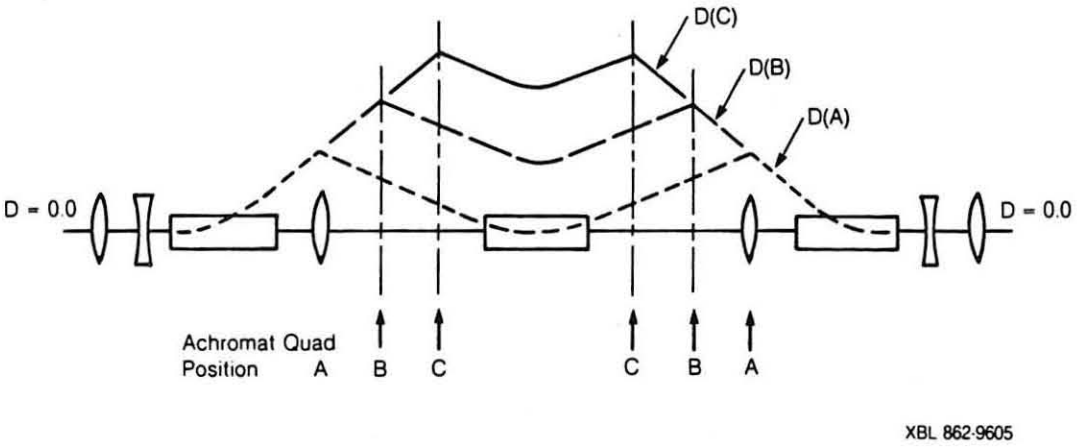

Fig. 13. TBA - Dependence of the matched dispersion function D on the position of the achromat quadrupoles. As the quadrupoles are moved from position A to C the strength required to match the dispersion function reduces.

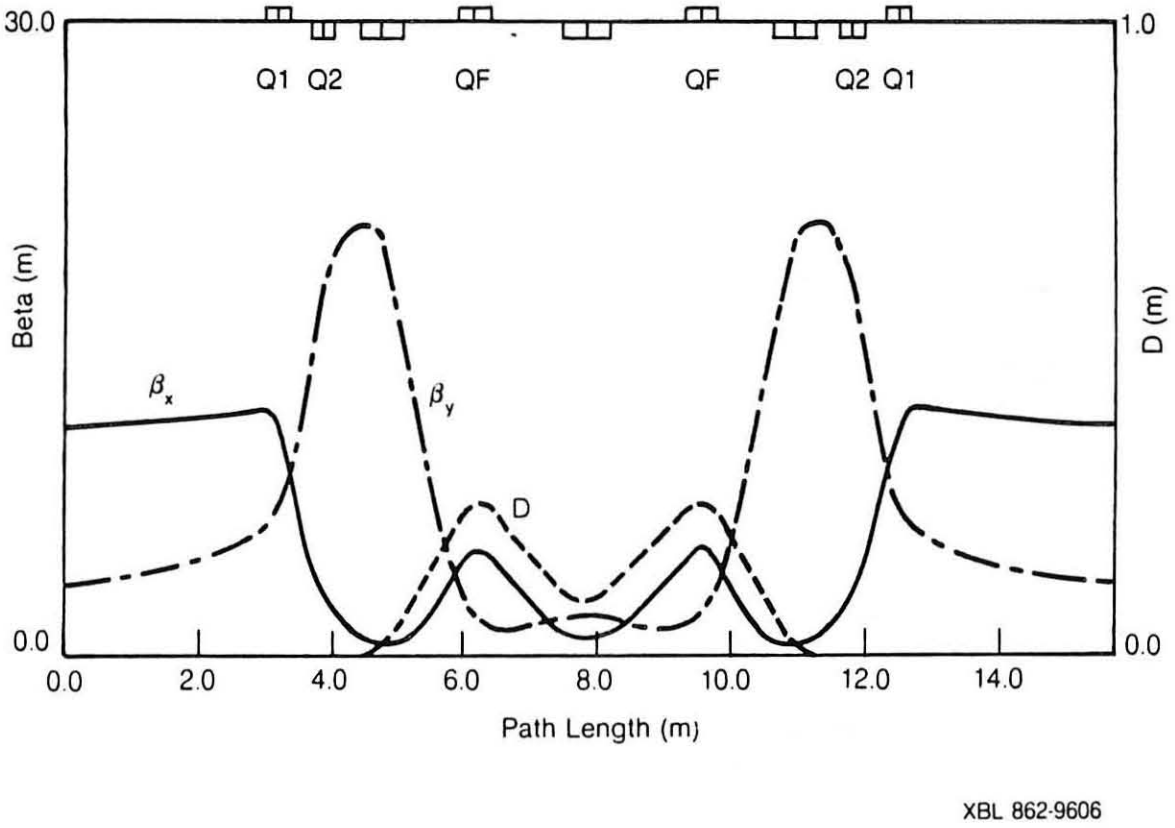

Fig. 14. TBA - Structure and lattice functions.

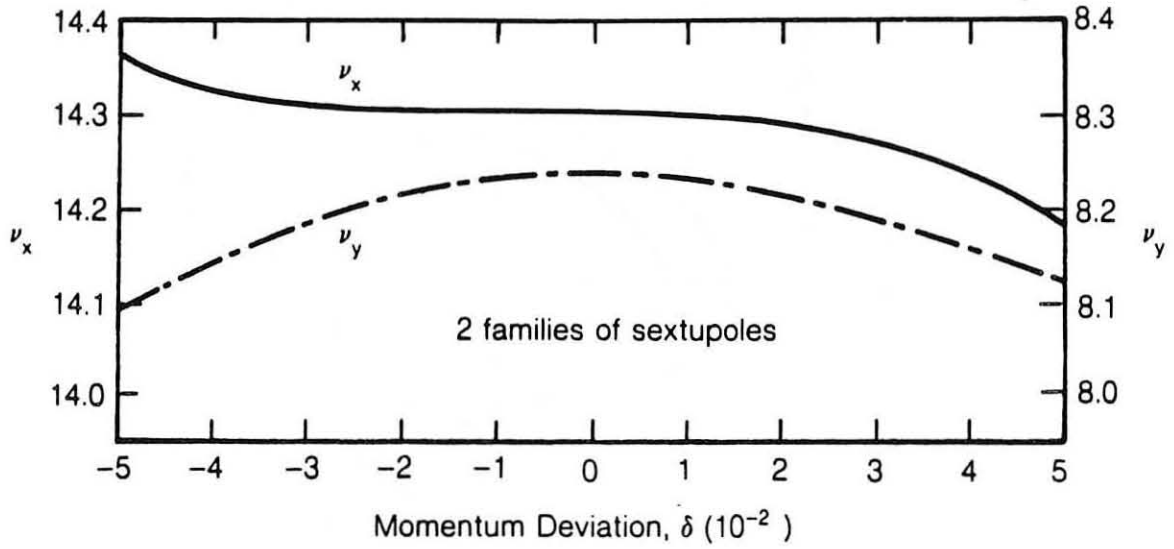

Fig. 15. TBA - Betatron tune as a function of momentum.

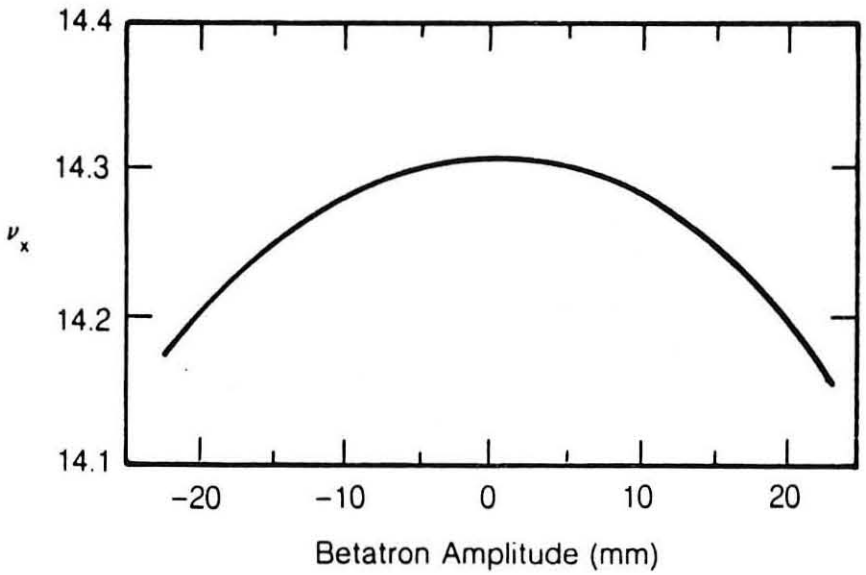

XBL 862-9607

Fig. 16. TBA - Radial tune shift with betatron amplitude, measured at the symmetry point in the insertion region.

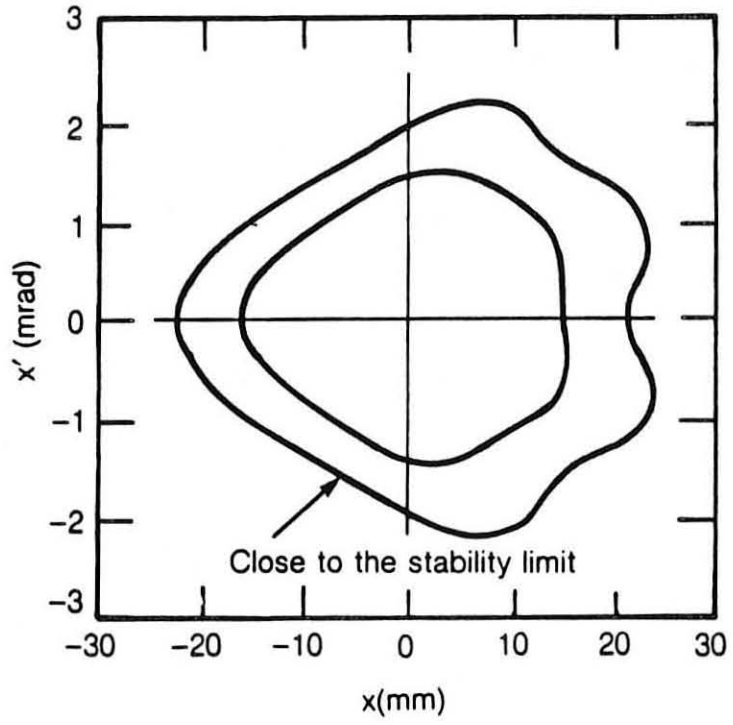

Fig. 17. TBA - Radial phase space trajectories.

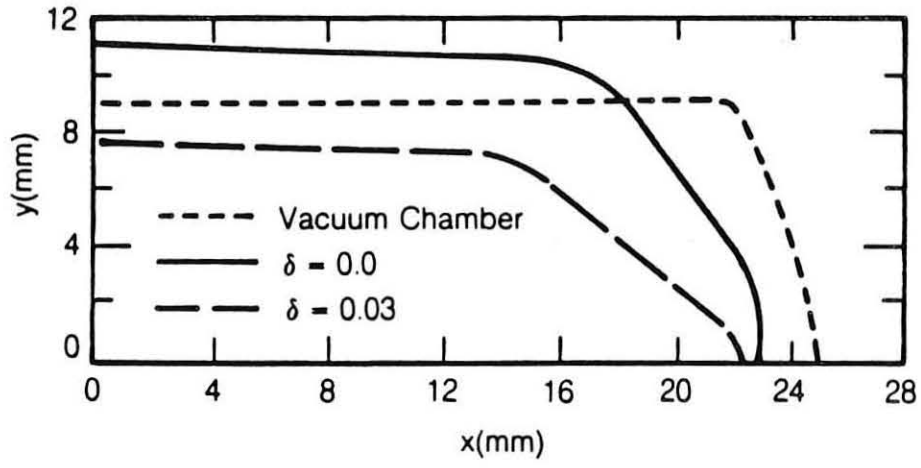

Fig. 18. TBA - dynamic aperture.

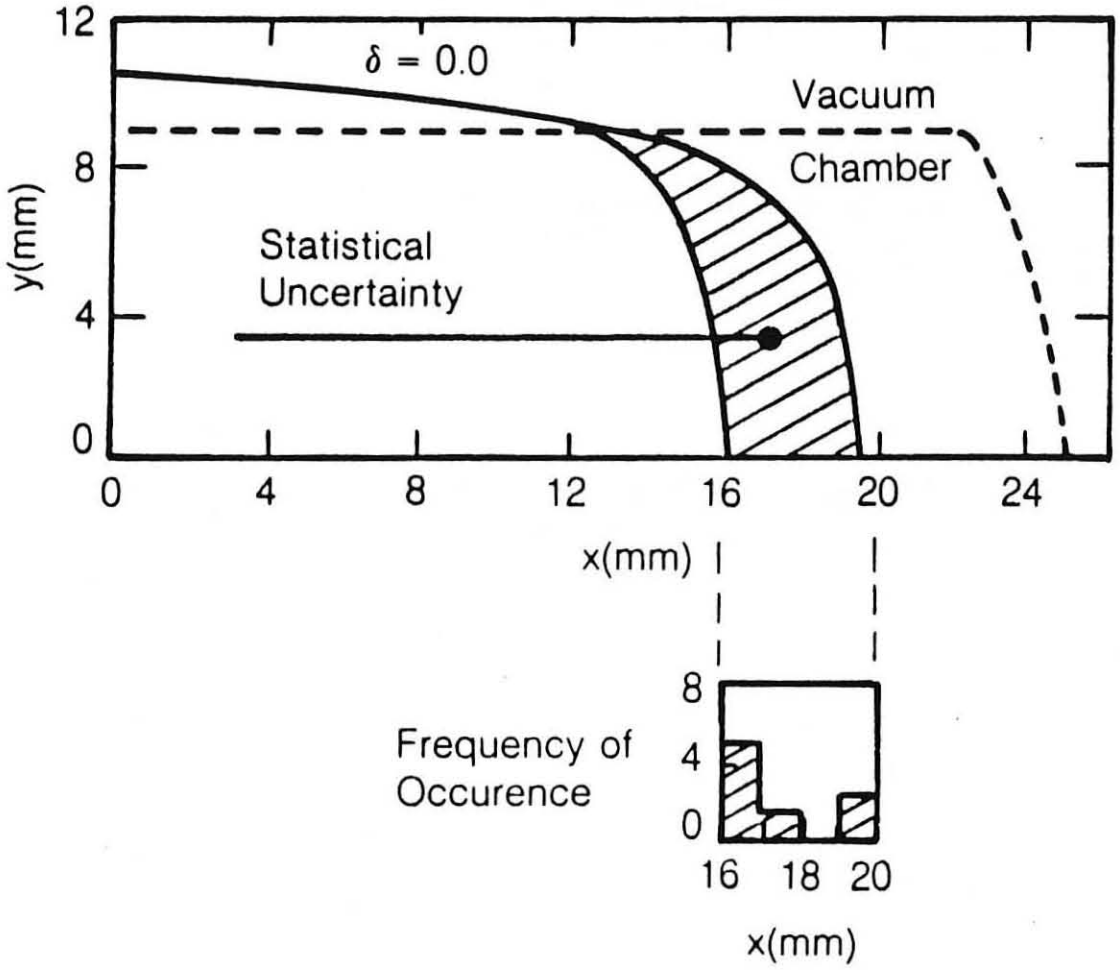

XBL 862-9609

Fig. 19. Dynamic aperture in the presence of magnetic field errors. The statistical uncertainty along the x-axis is shown.

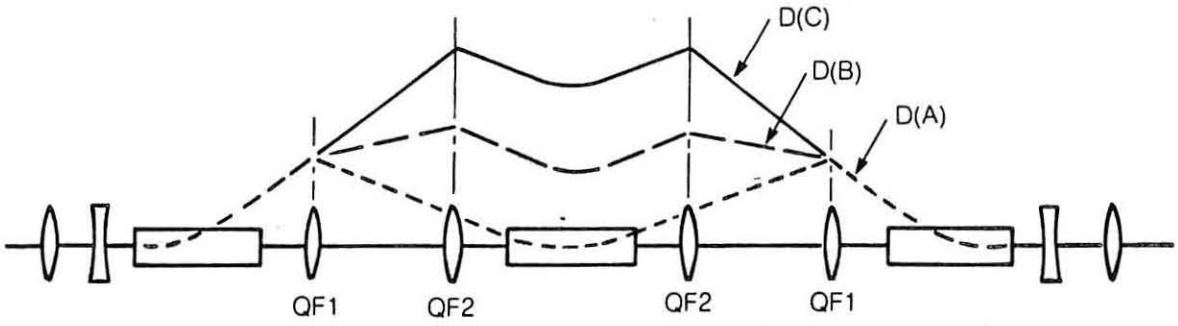

Fig. 20. TBA with two families of achromat quadrupoles. By differentially powering QF1 & QF2 it is possible to create the same dispersion in the central bend as those shown in Fig. 12.

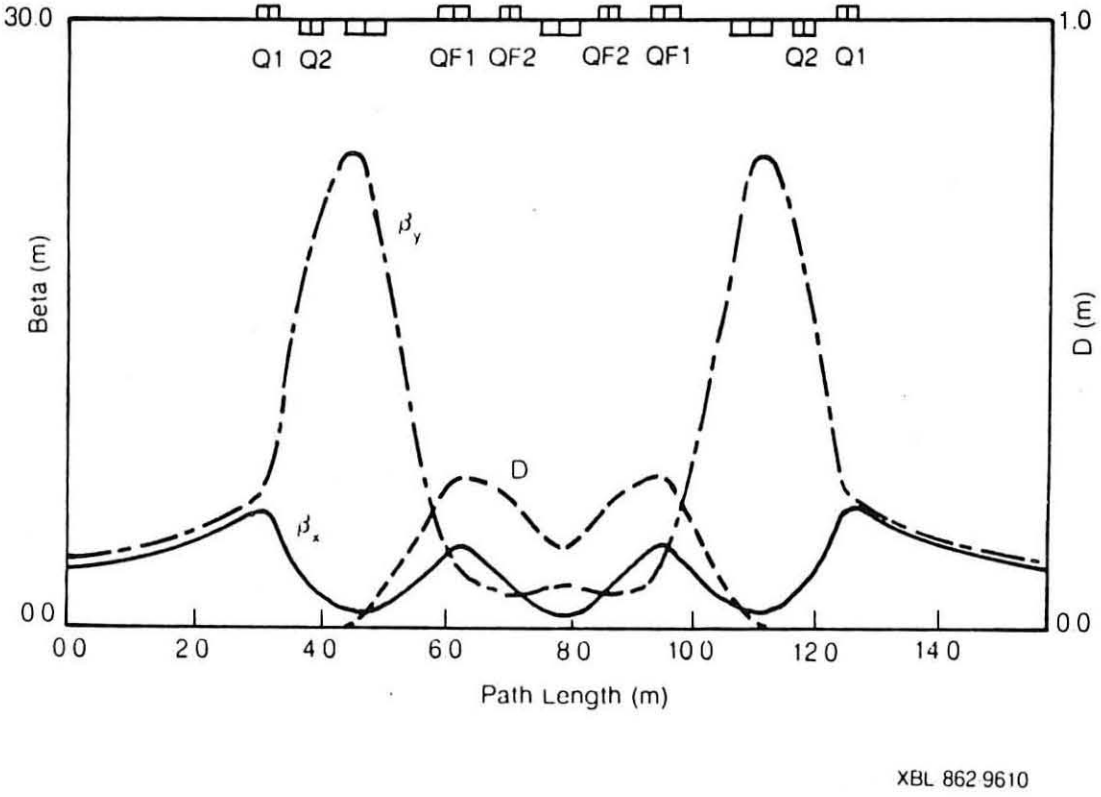

Fig. 21. TBA with two quadrupole families/achromat.

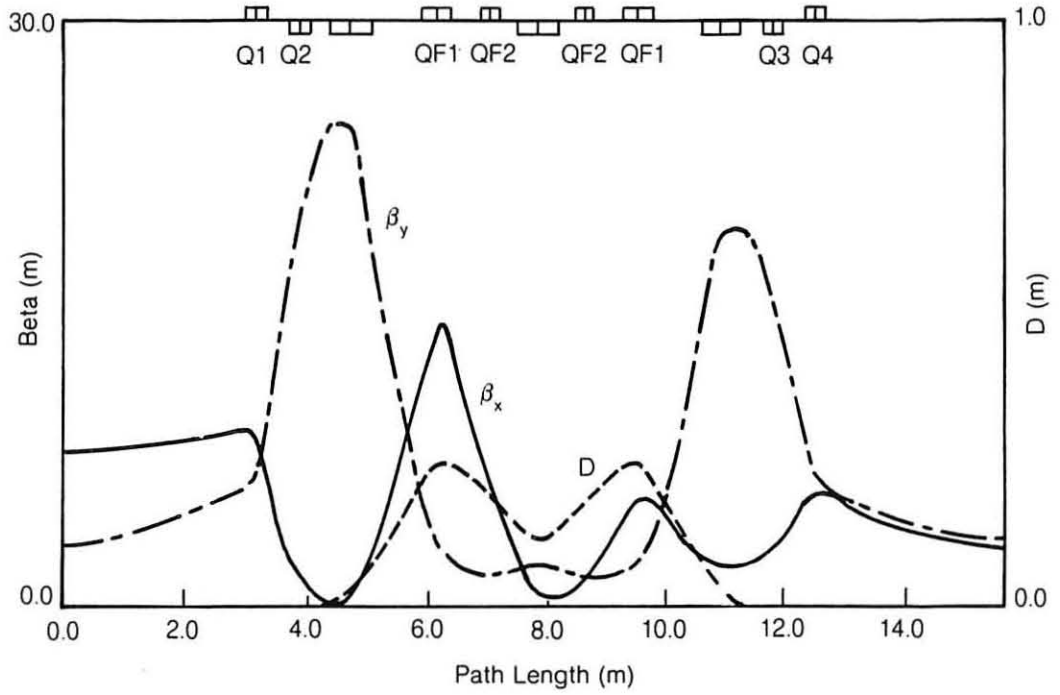

Fig. 22. TBA with β_x tuned to different values in alternate straight sections.

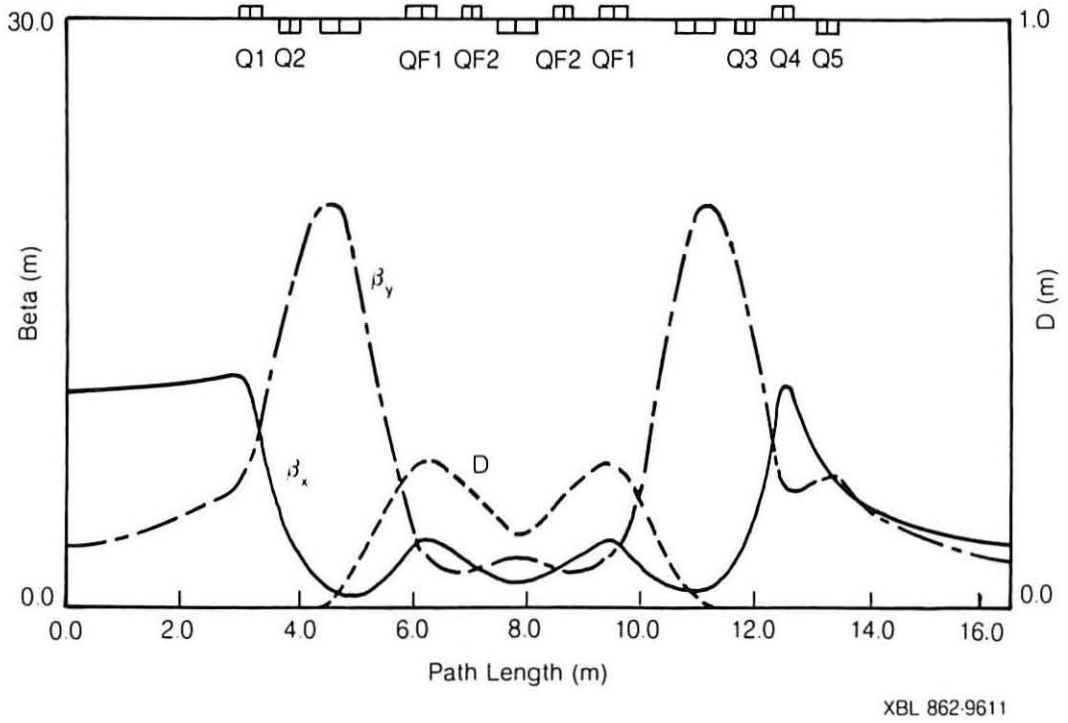

Fig. 23. TBA employing triplet matching in alternate straight sections.